RSC Advances

COMMUNICATION

View Article Online
View Journal | View Issue

Cite this: *RSC Adv.*, 2015, **5**, 16549

Robust transparent mesoporous silica membranes as matrices for colorimetric sensors†

Donghun Kim and Bradley F. Chmelka*

Received 12th September 2014
Accepted 28th January 2015

DOI: 10.1039/c4ra10339d

www.rsc.org/advances

Transparent functionalized mesoporous silica membranes have been prepared with high surface areas (~500 m^2 g^{-1}) that exhibit high sensitivities for colorimetric detection and sensing of dilute heavy-metal ions (*e.g.*, Pb^{2+}).

Colorimetric receptors incorporated into high-surface-area materials provide simple, inexpensive, and sensitive ways to detect dilute pollutants or toxicants in waste water or surface-water run-off.[1,2] Calcined polymeric-surfactant-directed mesoporous silica materials are attractive host materials for such applications, as they possess high surface areas, relatively large pores, uniform pore-size distributions, and excellent hydrothermal stabilities.[3–5] Mesostructured surfactant-silica composite materials can be prepared with high transparencies and, with the incorporation of photo-responsive functionalities,[6] have been extensively utilized for optical applications[7] (*e.g.*, sensors,[8] Bragg reflectors,[9] non-linear optical materials,[10] molecular probes,[11] and wave-guides[12]). These typically have relied on co-assembly of the photo-responsive molecules with the surfactant and inorganic precursor species, which form non-porous composite materials. For chemical sensing applications, the surfactant species must be thoroughly removed (*e.g.*, by calcination) to allow analyte species to diffuse to colorimetric receptors functionalized onto the internal mesopore surfaces.[2] However, such materials often suffer from insufficient mechanical robustness, as manifested by undesirable closure of the mesopores[13] and/or formation of microcracks,[5,14] during removal of the surfactant structure-directing agents. Therefore, as membranes or monoliths, they are often opaque and have limited uses for optical applications, including as sensors, because of the need to collect and analyze scattered light, which significantly reduces sensitivity. High extents of silica cross-linking prior to co-assembly with polymeric surfactants have been used to reduce the volume contraction of silica frameworks during calcination and yield transparent mesoporous silica "plates", although possessing relatively-small pore sizes[15] and/or significantly-reduced degree of mesostructural ordering,[16] which are expected to have deleterious effects on mass transport in the materials. Improvements in the mechanical properties of mesostructured silica have been achieved by hydrothermal treatments before calcination,[17] however, osmotic stresses often lead to macroscopic cracking that damage the structural integrities of the membranes. Consequently, the thicknesses of transparent surfactant-directed mesoporous silica membranes have typically been restricted to micron-length-scales (*e.g.*, thin films[18] or powders[19,20]) as host materials for optically-responsive functionalities.

Transparent functionalized mesoporous silica membranes of arbitrary thicknesses (>1 μm) are desirable, because they allow much higher net amounts of functional groups and therefore are expected to provide significantly higher net sensitivities. Here, we report a protocol to improve the mechanical robustness of mesostructured silica frameworks without micro- or macro-cracking, which yield a novel combination of material properties, including high surface areas (~500 m^2 g^{-1}), relatively-large and uniform pore-size distributions, high pore connectivities, and excellent visible-light transparencies for calcined mesoporous silica membranes. Upon functionalization with dithizone, such membranes are demonstrated to be sensitive colorimetrically to dilute heavy-metal ions (*e.g.*, ~20 ppb Pb^{2+}).

Free-standing mesoporous silica membranes with cubic, intermediate, or hexagonal mesostructures were prepared with surface areas ~0–700 m^2 g^{-1} that are highly dependent on mesopore periodicities and post-synthesis treatment conditions. Free-standing mesostructured silica membranes were synthesized by co-assembly of non-ionic triblock-copolymer

Department of Chemical Engineering, University of California, Santa Barbara, California, 93106-5080, USA. E-mail: bradc@engineering.ucsb.edu

† Electronic supplementary information (ESI) available: Detailed synthesis and characterization procedures and additional characterization results for the materials, including XRD patterns, HR-TEM images, N_2 sorption isotherms, solid-state single-pulse ^{29}Si MAS NMR spectra, nano-indentation measurements, UV/Vis spectra, and pycnometry measurements. See DOI: 10.1039/c4ra10339d

(Pluronic™ F127) and hydrolyzed network-forming molecular silica precursors during evaporation of volatile solvents[17] (see ESI,† for detailed synthesis and characterization procedures, mesostructural ordering, Fig. S1, and porosities, Fig. S2†). As-synthesized membranes without or with exposure to water vapor at 80 °C were subsequently calcined to remove the surfactant species and thereby generate porosity. The surface areas of the resulting membrane materials were established from N_2 sorption isotherms acquired at 77 K by using the Brunauer–Emmett–Teller (BET) method (Fig. 1). The surface areas of water-vapor-treated and calcined mesoporous silica membranes were determined to be in the range of 500–700 $m^2\ g^{-1}$ (pore diameters ~8 nm), which are correlated with mesopore periodicities and are much higher than those (0–350 $m^2\ g^{-1}$) measured for calcined mesoporous silica membranes prepared without water-vapor treatments. This indicates that water-vapor treatments have improved the thermal stabilities of mesostructured silica membranes and therefore yield significantly higher surface areas, compared to non-water-vapor-treated and calcined membranes. Such enhanced stability is consistent with an increased extent of fully-cross-linked (Q^4) silica species after water-vapor treatment, established by quantitative solid-state single-pulse ^{29}Si magic-angle-spinning NMR spectroscopy (Fig. S3 and Table S1, ESI†). Additionally, improved thermal stabilities induced by water-vapor treatments for mesostructured silica membranes are also correlated with increased mechanical robustnesses. Nano-indentation measurements for as-synthesized cubic mesostructured silica membranes without and with water-vapor treatments (Table S2, ESI†) establish that water-vapor treatments lead to improved membrane hardnesses from 180 MPa to 500 MPa. Thus, water-vapor treatments yield improved thermal and mechanical stabilities of mesostructured silica membranes without inducing cracking. This enables the membrane shapes to be maintained, along with the preparation of large-size (at least 3 × 3 cm^2) calcined mesoporous silica membranes (Fig. 2f).

Pore connectivities of the calcined mesoporous silica membranes can be controllably mediated by using water-vapor treatments to prevent or allow pore closure. Calcined cubic mesoporous silica membranes (F127/TEOS molar ratios 0.004–0.006) prepared without water-vapor treatment exhibited very-low BET surface areas (<1 $m^2\ g^{-1}$, Fig. 1), indicating low porosities that are inaccessible to N_2 molecules. Nevertheless, SAXS patterns and HR-TEM images (Fig. 2a and c) for a calcined cubic mesoporous silica membrane prepared with a F127/TEOS molar ratio of 0.004 establish that the membrane maintained a cubic mesostructure after calcination. This suggests that the very-low BET surface areas for calcined cubic mesoporous silica membranes are due to closure of mesopore necks during calcination, which was previously observed for cubic mesoporous silica powders after high-temperature treatment (*e.g.*, 900 °C).[13] By comparison, without water-vapor treatment, closure of mesopore necks in cubic mesoporous silica membranes is shown here to occur even at modest calcination temperature of 550 °C, which reflects the insufficient thermal stabilities of the non-water-vapor-treated mesostructured frameworks. This is also manifested by large lattice contractions (28%) after calcination established by SAXS measurements for non-water-vapor-treated as-synthesized (Fig. S1, ESI†) and calcined cubic silica membranes (Fig. 2a). By comparison,

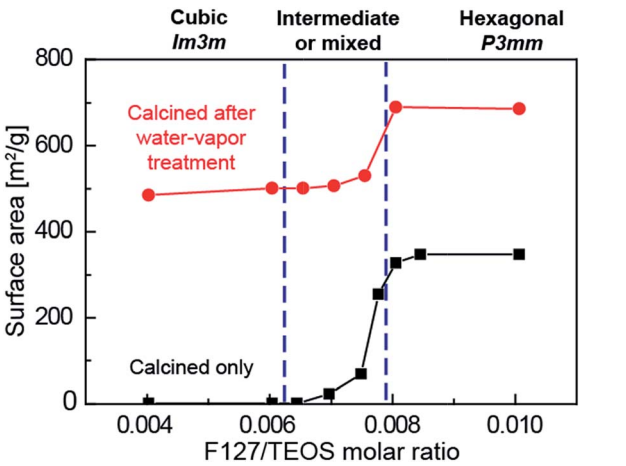

Fig. 1 Surface areas of calcined mesoporous silica membranes synthesized initially with different molar ratios of the structure-directing surfactant and silica precursor species (F127/TEOS) without and with post-synthesis treatments with water vapor at 80 °C. The dashed lines indicate approximate regions over which mesostructural ordering is intermediate between the cubic and hexagonal phases.

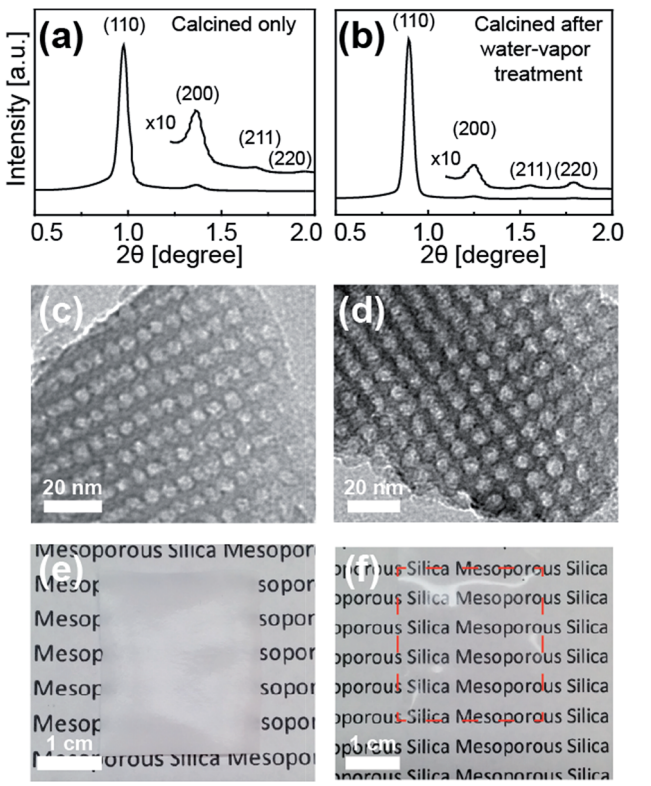

Fig. 2 (a and b) Small-angle X-ray scattering patterns, (c and d) TEM images, and (e and f) optical images for calcined mesoporous silica membranes (0.004 F127/TEOS molar ratio) synthesized (a, c and e) without and (b, d and f) with water-vapor treatments, respectively.

water-vapor-treated as-synthesized silica membranes result in a ~20% contraction (Fig. 2b), while manifesting almost identical cubic mesostructural order in high-resolution TEM images (Fig. 2c and d). Notably, the water-vapor-treated membranes remain micro-crack-free even for free-standing membranes thicker than 200 μm, which are highly transparent (Fig. 2f). UV/Vis spectra (Fig. S4, ESI†) of an as-synthesized mesostructured silica membrane (thickness ~150 μm) and water-vapor-treated and then calcined mesoporous silica membrane (thickness ~120 μm) establish their high transparencies for visible light (>90% between 300 and 700 nm). While conventional hydrothermal treatment can provide crack-free surfactant-directed mesoporous silica thin films up to ~1 μm thickness,[17] the synthesis method described here allows preparation of crack-free mesoporous silica membranes with more than two orders of magnitude greater thickness, which is enough to be free-standing.

Thermally-induced mesopore closure due to insufficient thermal stabilities can yield high volume fractions of closed mesopores in calcined mesoporous silica membranes. Mesoporous silica membranes prepared with F127/TEOS ratios between 0.004 and 0.010 were calcined without water-vapor treatment to allow closure of mesopores, and their volume fractions of closed and open pores were determined, based on the accessibility of N_2 molecules by using pycnometry and N_2 sorption experiments. The calcined cubic mesoporous silica membranes were measured to possess high overall volume fractions of closed mesopores and very-low volume fractions of open mesopores, which are consistent with their low BET surface areas. For example, calcined cubic mesoporous silica membranes prepared with 0.006 F127/TEOS molar ratio exhibit 0.27 and 0.03 for closed- and open-pore volume fractions, respectively, with the balance being the silica frameworks (Fig. S5, ESI†). By comparison, calcined mesoporous silica membranes prepared with higher F127/TEOS molar ratios of 0.008–0.010 possess open-mesopore volume fractions of 0.30–0.45, while still containing closed mesopores that diminish in volume fraction from 0.26 to 0.14. The presence of closed mesopores in hexagonal mesoporous silica membranes is consistent with increased BET surface areas for the water-vapor-treated mesoporous silica membranes prepared with F127/TEOS molar ratios between 0.004 and 0.010.

The high mechanical robustnesses of the membranes with closed mesopores, compared to those with open mesopores, were corroborated by nano-indentation measurements. The hardnesses were determined from load-depth curves recorded for cubic mesostructured silica membranes (F127/TEOS molar ratio of 0.004) prepared under identical conditions without and with water-vapor treatment and subsequent calcination at 550 °C to yield materials with closed and open mesopores, respectively. Despite the presence of micro-cracks, a calcined cubic mesoporous silica membrane with closed mesopores yielded a higher hardness (5.4 GPa) than that with open mesopores (2.3 GPa), which corroborates the advantages of closed mesopores (Table S2, ESI†). Such materials with high volume fractions of closed pores are attractive as low-dielectric-constant materials, due to their impermeabilities and the low dielectric constant of air (~1).[21,22]

The combination of high transparencies and high surface areas of mesoporous silica membranes prepared with water-vapor treatments is attractive for sensing applications that exploit the sensitivity of colorimetric functional species grafted onto internal mesopore surfaces of the membranes. In addition, the high transparencies of the membranes also allow use of UV/Vis transmission spectroscopy, which can be used to determine the absolute amounts of colorimetric functional moieties that are present, based on the Beer–Lambert law. This has previously been challenging for conventional calcined polymeric-surfactant-directed mesoporous silica materials, which are typically opaque and result in low transmitted light intensities, due to scattering losses.[23] For example, conventional mesoporous silica powder and transparent mesoporous silica membranes functionalized with dithizone, which is a widely-used organic material for detection or separation of heavy-metal ions (*e.g.*, Pb^{2+}),[24] were exposed to pH-7 buffer solutions containing 0 or 1 ppm Pb^{2+} ions, and their UV/Vis transmittance spectra were acquired (Fig. S6, ESI†). Dithizone-functionalized mesoporous silica powder exhibited very-low transmittance in the visible-light range, due to significant scattering, and consequently absorbances for dithizone functionalities could not be resolved. Low signal sensitivity precluded detection of Pb^{2+} ions, which typically requires advanced instrumentation (*e.g.*, an integrating sphere)[20] to collect scattered light signals to obtain sufficient signal intensities.

In contrast, the high transparencies of the dithizone-functionalized mesoporous silica membranes allow light-absorbance changes upon exposure to Pb^{2+} ions to be sensitively detected by using UV/Vis transmission spectroscopy. In the absence of Pb^{2+} ions, the dithizone-functionalized membrane yields strong absorption intensities at 424 and 586 nm (Fig. 3a), which manifest interactions between dithizone molecules and the silica support.[25] The dithizone loading in a 1 cm^2 × 120 μm-thick transparent mesoporous silica membrane was determined to be ~1 nmol, based on optical density measurements and analyses that used an extinction coefficient of 21 400 cm^{-1} M^{-1} at 450 nm.[26] This relatively low dithizone loading balanced resolution and sensitivity considerations for detection of dilute Pb^{2+} ions (*e.g.*, 20 ppb). After exposure to Pb^{2+} ions, a displacement of the absorption intensity maximum to 505 nm is observed (Fig. 3a), due to formation of dithizone–Pb^{2+} complexes.[4] This is consistent with a similar displacement of absorption intensity (*e.g.*, 620 nm *versus* 520 nm) that has been reported for dithizone in tetrachloromethane without and with Pb^{2+} ions, respectively.[26]

Moreover, high transparencies of the membranes also allow additional intensification of the absorption signals by overlaying several membranes for UV/Vis transmission spectroscopy measurements. Fig. 3a shows UV/Vis absorbance spectra for 5-overlain dithizone-grafted mesoporous silica membranes exposed to a pH-7 buffer containing 0–1000 ppb Pb^{2+} ions that collectively exhibit greater intensity than for a single membrane. The resulting absorbance changes upon exposure to Pb^{2+} ions manifested distinct color changes that were visually perceptible to the naked eye, even for very dilute Pb^{2+} ions (*e.g.*, 20 ppb, Fig. 3b). The absorbance change at 505 nm exhibits a

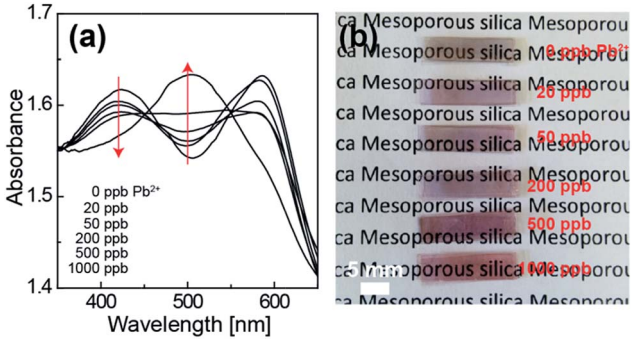

Fig. 3 (a) UV/Vis absorbance spectra and (b) images of five stacked 120 μm-thick dithizone-functionalized transparent mesoporous silica membranes exposed to pH 7 buffer solutions containing 0–1000 ppb of Pb^{2+} ions. The arrows in (a) indicate increasing Pb^{2+} concentration. The scale bar in (b) represents 5 mm.

linear correlation with the Pb^{2+}-ion concentration of the buffer solution in a range of 20–1000 ppb (Fig. S7, ESI†). This enables quantitative determination of Pb^{2+} ions without significant calibration efforts, due to the linear dependence of the absorbance on the amount of colorimetric functional moieties present, as well as controllable light-path lengths (*e.g.*, membrane thicknesses).

To summarize, we have prepared robust and transparent mesoporous silica membranes with high surface areas that have been demonstrated to be attractive host materials to incorporate colorimetric functional moieties for sensing applications. While insufficient thermal stabilities of polymeric-surfactant-directed mesostructured silica membranes invariably result in micro-cracks and/or closed mesopores upon calcination, water-vapor treatments improved the stabilities of the silica frameworks, therefore enabling the preparation of highly transparent mesoporous silica membranes with high BET surface areas. In particular, the high transparencies allow the absorbances of dithizone-functionalized mesoporous silica membranes to be assessed by using UV/Vis transmission spectroscopy, which enables quantitative determination of dilute-concentration Pb^{2+} ions (20–1000 ppb). These materials exhibit a novel combination of high surface areas, relatively-large pores with narrow pore size distributions, and high transparencies upon grafting with various colorimetric-sensing functional moieties that are expected to provide facile and inexpensive means for environmental monitoring of pollutants.

Acknowledgements

This work was supported in part by the Institute for Multi-scale Materials Studies at Los Alamos National Laboratory (UC Santa Barbara Contract #113144), the Institute for Collaborative Biotechnologies (contract no. W911NF-09-D-0001) from the USARO, and by AmberWave, Inc. The content does not necessarily reflect the position or the policy of the U.S. government and no official endorsement should be inferred. Characterization measurements were performed using the Central Facilities of the UCSB Materials Research Laboratory supported by the MRSEC Program of the NSF (DMR 1121053).

Notes and references

1 K. Singh, D. Sareen, P. Kaur, H. Miyake and H. Tsukube, *Chem.–Eur. J.*, 2013, **19**, 6914–6936; W. S. Han, H. Y. Lee, S. H. Jung, S. J. Lee and J. H. Jung, *Chem. Soc. Rev.*, 2009, **38**, 1904–1915; N. A. Carrington, G. H. Thomas, D. L. Rodman, D. B. Beach and Z.-L. Xue, *Anal. Chim. Acta*, 2007, **581**, 232–240.

2 A. Walcarius and M. M. Collinson, *Annu. Rev. Anal. Chem.*, 2009, **2**, 121–143.

3 D. Y. Zhao, J. L. Feng, Q. S. Huo, N. Melosh, G. H. Fredrickson, B. F. Chmelka and G. D. Stucky, *Science*, 1998, **279**, 548–552; D. Y. Zhao, Q. S. Huo, J. L. Feng, B. F. Chmelka and G. D. Stucky, *J. Am. Chem. Soc.*, 1998, **120**, 6024–6036; B. J. Melde, B. J. Johnson and P. T. Charles, *Sensors*, 2008, **8**, 5202–5228.

4 T. Balaji, S. A. El-Safty, H. Matsunaga, T. Hanaoka and F. Mizukami, *Angew. Chem., Int. Ed.*, 2006, **45**, 7202–7208.

5 S. A. El-Safty, D. Prabhakaran, A. A. Ismail, H. Matsunaga and F. Mizukami, *Adv. Funct. Mater.*, 2007, **17**, 3731–3745.

6 R. Hernandez, A.-C. Franville, P. Minoofar, B. Dunn and J. I. Zink, *J. Am. Chem. Soc.*, 2001, **123**, 1248–1249.

7 B. J. Scott, G. Wirnsberger and G. D. Stucky, *Chem. Mater.*, 2001, **13**, 3140–3150; C. A. Steinbeck, M. Ernst, B. H. Meier and B. F. Chmelka, *J. Phys. Chem. C*, 2008, **112**, 2565–2573; F. Hoffmann, M. Cornelius, J. Morell and M. Fröba, *Angew. Chem., Int. Ed.*, 2006, **45**, 3216–3251; C. Sanchez, B. Lebeau, F. Chaput and J. P. Boilot, *Adv. Mater.*, 2003, **15**, 1969–1994.

8 O. B. Miled, D. Grosso, C. Sanchez and J. Livage, *J. Phys. Chem. Solids*, 2004, **65**, 1751–1755.

9 M. C. Fuertes, F. J. López-Alcaraz, M. C. Marchi, H. E. Troiani, V. Luca, H. Míguez and G. J. A. A. Soler-Illia, *Adv. Funct. Mater.*, 2007, **17**, 1247–1254.

10 P. Innocenzi and B. Lebeau, *J. Mater. Chem.*, 2005, **15**, 3821–3831.

11 B. Dunn and J. I. Zink, *Acc. Chem. Res.*, 2007, **40**, 747–755; A.-C. Franville, B. Dunn and J. I. Zink, *J. Phys. Chem. B*, 2001, **105**, 10335–10339.

12 F. Marlow, M. D. McGehee, D. Zhao, B. F. Chmelka and G. D. Stucky, *Adv. Mater.*, 1999, **11**, 632–636; P. Yang, G. Wirnsberger, H. C. Huang, S. R. Cordero, M. D. McGehee, B. Scott, T. Deng, G. M. Whitesides, B. F. Chmelka, S. K. Buratto and G. D. Stucky, *Science*, 2000, **287**, 465–467.

13 M. Kruk and C. M. Hui, *J. Am. Chem. Soc.*, 2008, **130**, 1528–1529.

14 H. F. Yang, Q. H. Shi, B. Z. Tian, S. H. Xie, F. Q. Zhang, Y. Yan, B. Tu and D. Y. Zhao, *Chem. Mater.*, 2003, **15**, 536–541.

15 R. Ryoo, C. H. Ko, S. J. Cho and J. M. Kim, *J. Phys. Chem. B*, 1997, **101**, 10610–10613; C. H. Ko, J. M. Kim and R. Ryoo, *Microporous Mesoporous Mater.*, 1998, **21**, 235–243.

16 S.-J. Lee, S. S. Park, S. H. Lee, S.-H. Hong and C.-S. Ha, *J. Nanosci. Nanotechnol.*, 2013, **13**, 7459–7466.

17 D. Zhao, P. Yang, N. Melosh, J. Feng, B. F. Chmelka and G. D. Stucky, *Adv. Mater.*, 1998, **10**, 1380–1385.
18 A. Quach, V. Escax, L. Nicole, P. Goldner, O. Guillot-Noël, P. Aschehoug, P. Hesemann, J. Moreau, D. Gourier and C. Sanchez, *J. Mater. Chem.*, 2007, **17**, 2552–2560; G. Wirnsberger, B. J. Scott and G. D. Stucky, *Chem. Commun.*, 2001, 119–120; E. Palomares, R. Vilar and J. R. Durrant, *Chem. Commun.*, 2004, 362–363.
19 M. Liong, J. Lu, M. Kovochich, T. Xia, S. G. Ruehm, A. E. Nel, F. Tamanoi and J. I. Zink, *ACS Nano*, 2008, **2**, 889–896; R. Métivier, I. Leray, B. Lebeau and B. Valeur, *J. Mater. Chem.*, 2005, **15**, 2965–2973; E. Kim, H. E. Kim, S. J. Lee, S. S. Lee, M. L. Seo and J. H. Jung, *Chem. Commun.*, 2008, 3921–3923.
20 T. Balaji, M. Sasidharan and H. Matsunaga, *Analyst*, 2005, **130**, 1162–1167.
21 W. Volksen, R. D. Miller and G. Dubois, *Chem. Rev.*, 2010, **110**, 56–110.
22 R. A. Pai, R. Humayun, M. T. Schulberg, A. Sengupta, J.-N. Sun and J. J. Watkins, *Science*, 2004, **303**, 507–510; B. D. Lee, Y. H. Park, Y. T. Hwang, W. Oh, J. Yoon and M. Ree, *Nat. Mater.*, 2005, **4**, 147–151.
23 F. Schael, O. Reich and S. Engelhard, *Int. J. Photoenergy*, 2002, **4**, 21–26.
24 W. A. de Oliveira and R. Narayanaswamy, *Talanta*, 1992, **39**, 1499–1503; A. Safavi and M. Bagheri, *Sens. Actuators, B*, 2004, **99**, 608–612; Y. Takahashi, S. Danwittayakul and T. M. Suzuki, *Analyst*, 2009, **134**, 1380–1385.
25 C. McDonagh, C. S. Burke and B. D. MacCraith, *Chem. Rev.*, 2008, **108**, 400–422.
26 O. A. Weber and V. B. Vouk, *Analyst*, 1960, **85**, 40–45.